OBSERVATIONAL CONSTRAINTS ON SOLAR WIND ACCELERATION MECHANISMS

Marcia Neugebauer
Jet Propulsion Laboratory
California Institute of Technology
Pasadena, CA 91109

ABSTRACT

A complete theoretical understanding of the acceleration of the solar wind must account for at least three types of solar wind flow: high-speed streams associated with coronal holes, low-speed boundary layer flows associated with sector boundaries, and both high- and low-speed flows associated with impulsive ejections from the Sun. The properties of each type of flow are summarized.

Types of Flow

Three types of solar wind flow are considered for the purpose of placing observational constraints on theories of solar wind acceleration. These are: the fast, hot flow from coronal holes, the slow, dense, cool flow near sector boundaries, and transient flows. This trichotomy is simply a convenient system for describing extremes of solar wind behavior, and should not imply that three and only three distinct theories of solar wind acceleration are required. A single steady state theory could perhaps explain both the hole and the boundary flows, but such a theory would have to include an explanation of the sharp latitude and longitude boundaries of high-speed streams from coronal holes (Rosenbauer et al., 1977; Schwenn et al., 1978). It is also possible that there are solar wind flows which are not included in this three-way classification. For example, Burlaga et al. (1978) and Levine (1978) have presented evidence for the existence of flows from magnetically open regions of the corona which are neither holes nor streamers. Even if such flows are important contributors to the solar wind, however, they are not included in this survey because their properties have not been determined.

The first transient flows to be identified were the driver gases behind interplanetary shocks. Their properties are discussed in the paper by Zwickl et al. in these Proceedings. Observations of coronal transients and mass ejections have led to a realization that there are transient inputs to the solar wind which are not associated with either flares or shocks. Approximately 70% are associated with eruptive prominences (Munro et al., 1979), many of which are not sufficiently energetic to yield an interplanetary shock.

Table 1 compares the properties of the several types of impulsively ejected plasma which I believe are really different manifestations of one class of plasma flow. The numbers in this table were either compiled from the referenced work or computed from King's (1977, 1979) Interplanetary Medium Data Tape (IMDT) using the authors' lists of event times. The composition and the thermal and magnetic properties of the differently named events are all quite similar. Transient flows occur in both the low-speed and the high-speed solar wind. Their plasma density is highly variable, both from event to event and within a single event. Most of the material added to the solar wind in transient events is the hot coronal material originating in a large region of space above a flare

Table 1. Properties of different manifestations of transient flows

Type:	He Enrichment	Anom low T_p	Low T_e	High Ionization	He^+	He Abund. Enhancements	Magnetic Clouds
Reference:	Hirshberg et al, 1972	Gosling et al, 1973	Montgomery et al, 1974	Bame et al, 1979 Fenimore, 1980	Schwenn et al, 1980 Zwickl et al, 1982	Borrini et al, 1982	Klein & Burlaga, 1982
Definition:	$\frac{n_\alpha}{n_p} \geq .15$	post shock $T_p < 2\times10^5 \times (\frac{v}{350} - 1)$	$T_e < 6\times10^4$	$T_{Fe} > 2.3 \times 10^6$	recognizable peak at M/Q = 4	$\frac{n_\alpha v_\alpha}{n_p v_p} \geq .10$	duration ~ 1 day B > 10 γ large ΔB_z
Speed, km/s range	358-655	411-612	345-616		360-500	281-674	318-665
average	546	532	478			434	417
n_p, cm^{-3} range		2.6-9.9	2.5-20		6.5-50	1.8-51	2.5-27
average		6	7			10	12
T_p, 10^4K		7	3	low in 43%	1.5-3	6	7
T_e, 10^4K			5	low in 43%			
n_α/n_p	.21(pk)	.18(pk)		43% > .09	.025-.094	>.10	
Ionization temp.				$T_{Fe} = 2.3-17\times10^6$	mixture	"Anom. high"	
Q_e, erg/cm^2s			~1x10^{-3}				
$B_\perp$, γ	11	6.8	7.3			8.5	10.6(pk = 12)
$\frac{B^2}{8\pi} + n_p kT_p$						local max	local max
$\beta = \frac{8\pi nkT_p}{B^2}$		0.3	0.3			0.2	0.2 - 0.5
Shock assoc.	75%	100%(def'n)	83%	27%	75%	44%	31%
Duration		≤36 h	10 - >40 hr		1-6 hr	~ 1 day	~ 1 day
No. events	12	12	13	14	4	73	45

site or an erupting prominence. A small fraction of the ejected mass is the much cooler prominence material itself, which can evidently pass through the corona without reaching ionization equilibrium with the surrounding gas. In this way both unusually high and unusually low ionization states, and sometimes mixtures of the two, can be associated with transient flows. The combination of high ionization state and low kinetic temperature suggests that the gas has been cooled by greater than average expansion and/or that heat conduction has been inhibited, perhaps by disconnection of the magnetic field from the Sun. The electron heat flux is less than usual, with both superthermal and energetic electrons streaming along the field nearly symmetrically towards and away from the Sun (Palmer et al., 1978; Bame et al., 1981). The picture which has emerged is that the magnetic topology is closed, either with the field closing on itself in a bubble configuration or with both ends of the field lines remaining attached to the Sun.

Correlations of solar wind observations with x-ray and EUV observations obtained by Skylab in 1973-4 indicated that coronal holes are the source of long-lived, high-speed solar wind streams (Krieger et al., 1973,1974; Nolte et al., 1976). Feldman et al. (1976; 1978) and Bame et al. (1977) have summarized the properties of those high-speed streams observed between 1971 and 1974 which

attained speeds > 650 km/s. These streams were broad, extending over solar longitudes ranging up to 159°; the average FWHM was 89 ±34°. At 1 AU, the plasma in these streams is less dense, much hotter, and has less helium than the plasma from impulsive ejections. The hour-to-hour variability of plasma parameters within these streams is also much less than in low-speed flows (Bame et al., 1977).

Comparison of coronal observations with solar wind data shows that the plasma in which long-lived sector boundaries are embedded probably originates in helmet streamers which separate the flows from neighboring coronal holes (Hansen et al., 1974). The coronal temperatures of boundary flows estimated by Feldman et al. (1981) from heavy ion charge states are consistent with streamer temperatures.

It has long been known that sector boundaries preferentially occur in low speed, low temperature, high density plasma (Wilcox and Ness, 1965; Ness et al., 1971). To this body of knowledge, Borrini et al. (1981) have added the observations that the helium abundance, the differential flow between alphas and protons, and the alpha to proton temperature ratio all reach local minima near sector boundaries.

The electron temperature, electron heat flux, break-point energy between the thermal and the nonthermal electron distributions, and the electron strahl strength all exhibit local minima at sector boundaries (Pilipp et al., 1981; Feldman et al., 1981). Helios data also show that the electron temperature at sector boundaries decreases adiabatically with distance from the Sun, unlike the electrons in high speed streams, which cool significantly more slowly. From these data, Pilipp et al. concluded that the field lines within the sector boundary have become disconnected from the Sun. On the other hand, the visual form of coronal streamers suggests an open magnetic topology. The postulated reconnection may occur only within the small scale, often complex structure of the sector boundary. Further evidence for reconnection associated with sector boundaries is presented below.

Figure 1 summarizes my categorization of different solar wind flows. It could be misleading to average solar-wind properties as a function of solar-wind speed (although I am one of many people who have done this in the past), because two or more different acceleration processes contribute to the sample at any speed.

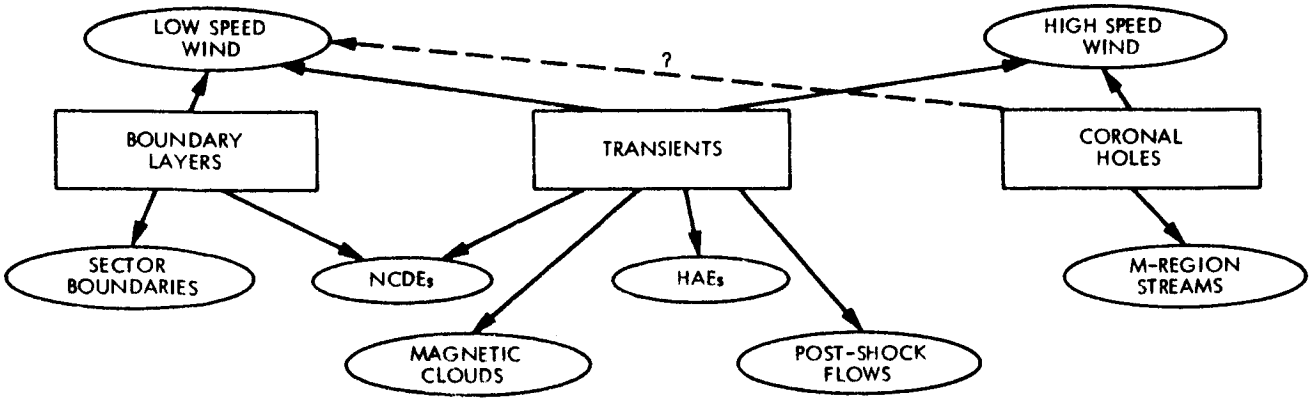

Figure 1. Suggested relation between various types of solar wind flow.

Comparison of Flow Properties

Figures 2 and 3 illustrate the similarities and the differences between the properties of the three different types of flow.

Transient flows are represented by a superposed epoch analysis centered on the onsets of the helium abundance enhancement events listed by Borrini et al. (1982). Many of the plots in Figures 2 and 3 nearly reproduce those given by Borrini et al., with some minor differences arising from my use of the IMDT rather than the Los Alamos data alone. Figures 2 and 3 contain several solar wind parameters which were not calculated by Borrini et al.

Boundary flows are represented in Figures 2 and 3 by a superposed epoch analysis around 45 sector boundary crossings observed between December, 1972, and September, 1975, during the period of low solar activity and recurrent streams from coronal holes. This time limitation was made in an effort to avoid inclusion of reversals of field direction associated with transient flows. For this reason, I have included fewer sector boundaries than were used in the study of Borrini et al. (1981). It is usually the case that, by the time it has reached 1 AU, the fast plasma from a coronal hole has overtaken the slower plasma from its leading sector boundary. There were 9 sector boundaries included in my sample for which the arrival of the leading edge of the high-speed stream was at least a day later than the passage of the sector boundary, a separate superposed epoch analysis was performed on these sector boundaries, and are labelled "no stream" in Figures 2 and 3.

Average properties of the high-speed streams from coronal holes are represented by horizontal lines on the right-hand side of the sector-boundary plots. The averages were computed by combining start and stop times of the high speed streams listed by Feldman et al. (1976) with the hourly average solar wind parameters from the IMDT. Feldman et al. corrected the data taken at 1 AU for the evolution of the high speed streams between 20 solar radii and 1 AU, but where there is overlap, my results agree with theirs within 20%.

Figure 2a shows superposed epoch plots of solar wind speed for ± 3 days around an HAE or a sector boundary. There is no obvious trend in the plot for HAE's; by 1 AU the transient plasma travels at the same speed as the ambient plasma. On the right side, one can see the low speed associated with sector boundaries as well as the increasing speed associated with the encroaching leading edge of the following coronal hole flow. The relative noisiness of the curve for HAEs compared to the "all" sector boundary curve arises from the combined effect of data gaps and the large range of speeds included in the sample.

Proton density is plotted in Figure 2b. The only trend associated with the transient events is the modest (30 %) increase several hours before the zero epoch time, probably indicating pile up of plasma ahead of the expanding transiently ejected plasma. Again, the event to event variance is large.

There is a definite density enhancement at sector boundaries. Comparison of the two curves on the right side of Figure 2b shows that a large part of the signal is, however, caused by the compression at the leading edge of the following high speed stream. The "no stream" data show two density peaks, one at the sector boundary and a larger one on the leading edge of the stream.

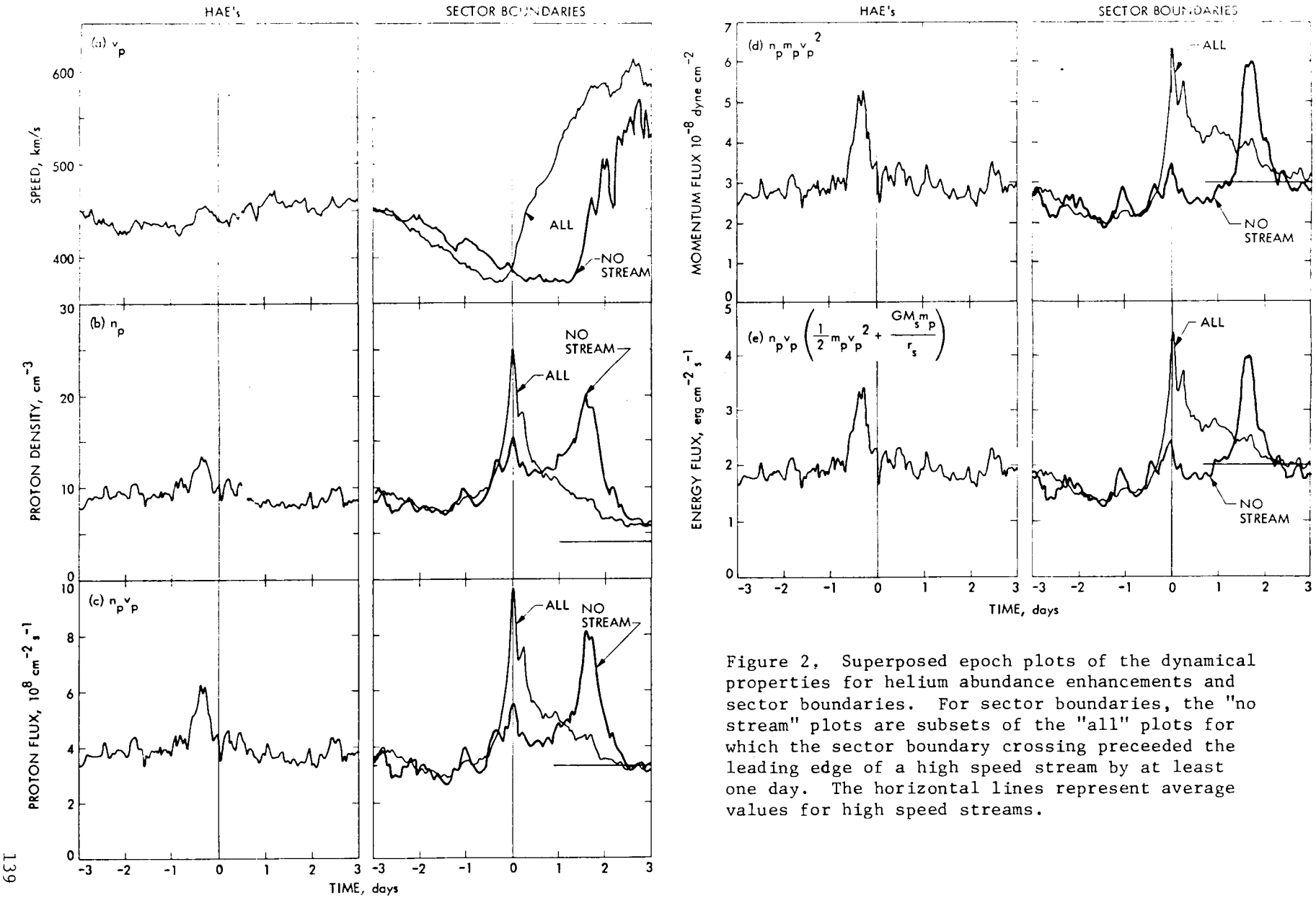

Figure 2. Superposed epoch plots of the dynamical properties for helium abundance enhancements and sector boundaries. For sector boundaries, the "no stream" plots are subsets of the "all" plots for which the sector boundary crossing preceeded the leading edge of a high speed stream by at least one day. The horizontal lines represent average values for high speed streams.

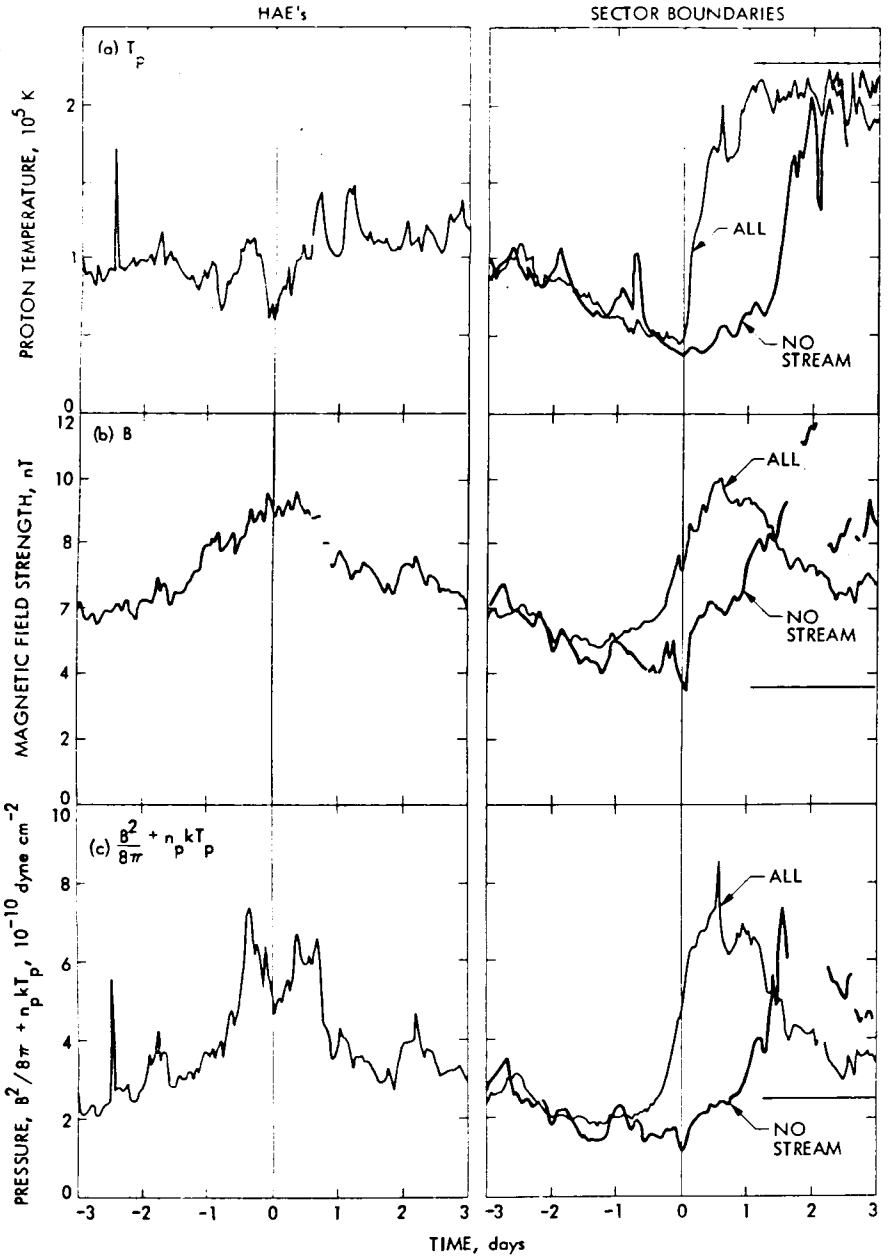

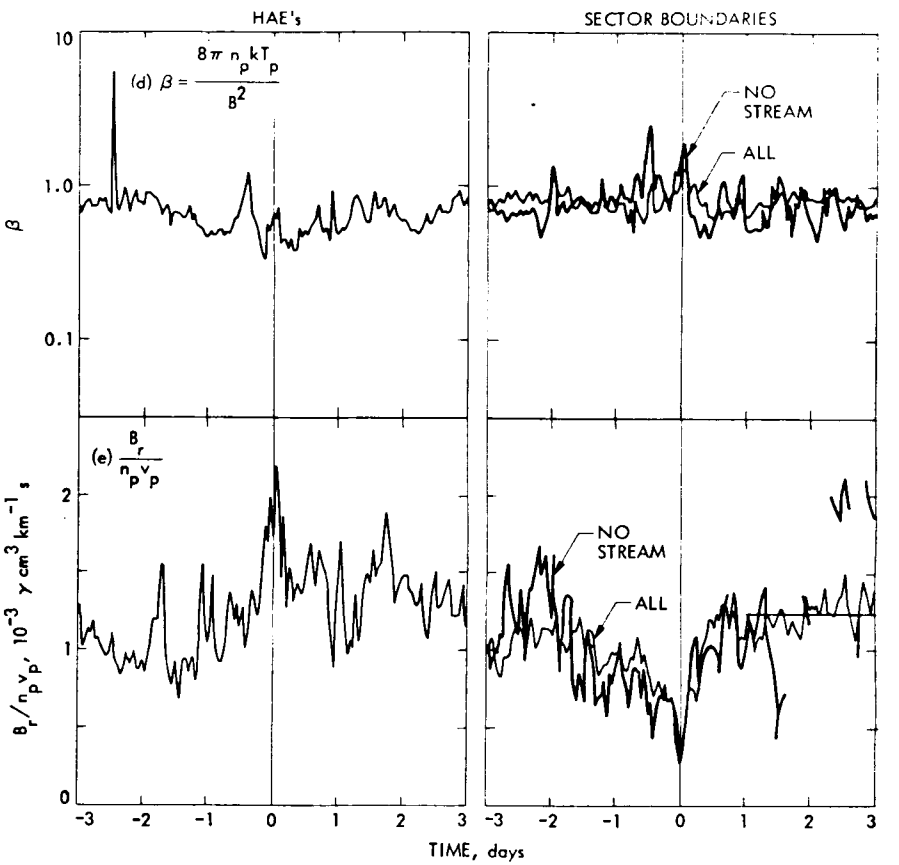

Figure 3. Superposed epoch plots of the thermal and magnetic properties for helium abundance enhancements and sector boundaries. For sector boundaries, the "no stream" plots are subsets of the "all" plots for which the sector boundary crossing preceeded the leading edge of a high speed stream by at least one day. The horizontal lines represent average values for high speed streams.

Figure 2c shows the product of density and speed, or the proton flux. The flux is roughly the same, $(4 \pm 1) \times 10^8$ cm^{-2} s^{-1}, for all three types of flow, and consistently less than in stream interaction regions.

The proton momentum flux ($n_p m_p v_p^2$) is plotted in Figure 2d. The values for the three different types of flow are remarkably similar, in agreement with studies by Steinitz and Eyni (1980) and Steinitz et al. (1982). The difference between my value of 3 dyne cm^{-2} (based primarily on IMP data) and the Steinitz et al. value of 2 dyne cm^{-2} (based on Mariner 2, Vela 3, and Helios data) may be largely explained by systematic differences between instruments. Density is the least accurately determined parameter; it could be in error by 30%, perhaps more. See Neugebauer (1982) for a discussion of the accuracy of solar wind measurements.

Figure 2e displays the variation of energy flux, $n_p v_p (m_p v_p^2/2 + m_p M_s G/r_s)$, where the second term accounts for the work done against solar gravity. The energy flux is close to 2 erg cm^{-2}s^{-1} for each of the three types of flow. The invariance of this parameter was not tested by Steinitz and coworkers.

Figure 3, in the same format as Figure 2, shows the distribution of internal energy in the plasma. Proton temperature (Figure 3a) reaches a minimum of about 5×10^4 K in both transient and boundary flows, as opposed to a very hot 2.3×10^5 K in coronal hole flows.

In Figure 3b, it can be seen that the magnetic field reaches a broad local maximum in transient flows and a narrow local minimum at sector boundaries. The field in coronal hole flow is similarly low.

The sum of the proton and magnetic pressures is plotted in Figure 3c, illustrating the local pressure maximum in transient flows mentioned earlier. Although the local minimum at sector boundaries is probably not statistically significant, it is possible that the plasma is locally falling into the sector boundary.

Figure 3d shows $\beta = 8\pi n_p k T_p / B^2$, which is lowest in the transient flows and highest at sector boundaries.

Finally, we consider the ratio $B_r/n_p v_p$, where B_r is the radial component of the interplanetary magnetic field. This ratio should be independent of distance from the Sun and unaffected by stream interactions if the field is frozen into the plasma and develops no kinks large enough to cause a local reversal of the sign of B_r. Figure 4 shows hourly averages of selected solar wind parameters for the solar rotation starting February 10, 1974. From top to bottom are plotted the solar wind speed, the logarithm of the proton flux, the logarithm of $B_r/n_p v_p$, and the longitude angle of the interplanetary magnetic field direction. The amplitude of the variation of $B_r/n_p v_p$ is about an order of magnitude greater than the amplitude of the variation of $n_p v_p$. Particularly noteworthy are the broad minimum in $B_r/n_p v_p$ around the sector boundary crossing on day 51 and the maximum near the HAE on day 53. The origin of the many small dips in $B_r/n_p v_p$ is still under investigation.

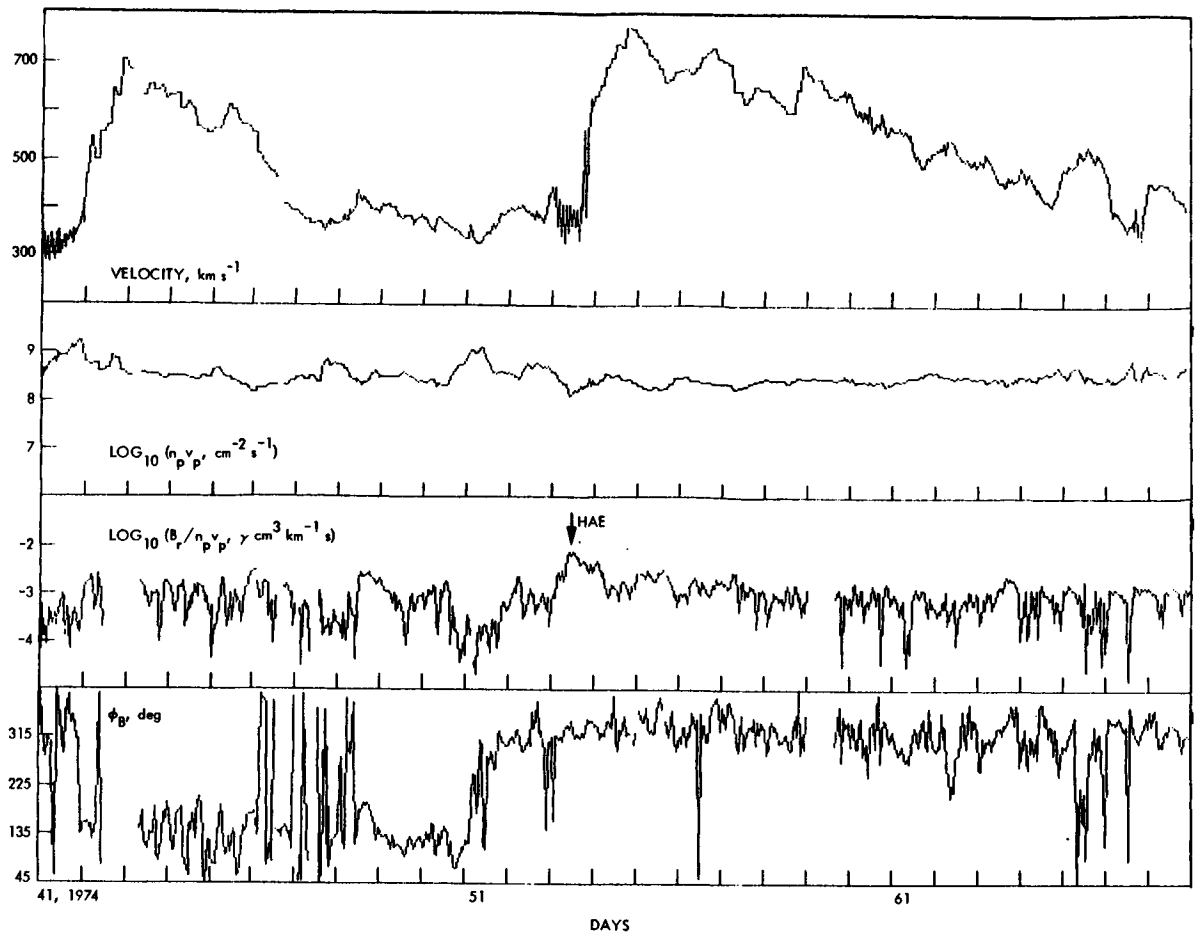

Figure 4. Hourly averaged data over one solar rotation to show the relation of variations in the parameter $B_r/n_p v_p$ to other solar wind features.

Superposed epoch plots of $B_r/n_p v_p$ for HAEs and sector boundaries are shown in Figure 3e. The similarity of the "all" and the "no stream" curves near the sector boundary is testimony to the invariance of this parameter through stream interactions. On the average, $B_r/n_p v_p$ peaks at about 2 (units of 10^{-3} γcm^{3}km^{-1}s) in HAEs, 1.2 in coronal hole flows, and reaches a minimum near 0.2 at sector boundaries. It is tempting to interpret the local minimum in $B_r/n_p v_p$ near sector boundaries as evidence for field line reconnection, in keeping with suggestions by Bavassano et al. (1976) and Pilipp et al. (1981).

Table 2 presents a numerical summary of the differences between the three types of flow. For those parameters plotted in Figures 2 and 3, the zero epoch values have been tabulated. Theories of solar wind acceleration must explain why fast, hot flows come from coronal holes while slow, cool boundary flows come from coronal streamers. There are probably some relevant clues in the ratios T_p/T_e, β, $n_a v_a/n_p v_p$, and $B_r/n_p v_p$ and in the ionization states of heavy ions.

After 20 years of solar wind observations, the number of question marks in Table 2 is remarkable. Different measurements of heavy ion ionization temperatures in high speed flow from coronal holes yield conflicting results (see Section 6 of paper by Bame, this Volume). Studies of anisotropies and

double streaming in high speed streams have not differentiated between transient and coronal hole flows; I have assigned these properties to flows from coronal holes, perhaps incorrectly.

Acknowledgements. I thank D. R. Clay for his help on this project. This research was conducted at the Jet Propulsion Laboratory of the California Institute of Technology under NASA contract NAS 7-100.

TABLE 2. Comparison of solar wind parameters in three types of flow

	HOLE	BOUNDARY	TRANSIENT
v, km/s	700	380	440
n, #/cm^3	4	15	10
nv, 10^8/cm^{2}s	3	5	5
nmv^2, dyne/cm^2	3	3	3
nm(mv^2/2 + mMG/r), erg/cm^{2}s	2	2	2
T_p, 10^5 K	2.3	0.7	0.6
T_e, 10^5 K	1.0	1.3	0.5
$n_\alpha v_\alpha / n_p v_p$	.05	.02	.10
Ionization temperatures			
T_O, 10^6 K	?	2.1	up to 3.4
T_{Fe}, 10^6 K	?	1.6	up to 17
Q_e, 10^{-3} erg/cm^2/s	3	<3	1
B, γ	6	3	9
Field topology	Open	?	Closed
$\beta = 8\pi k T_p / B^2$	1	2	0.3
B_r/nv, 10^{-3} γ cm^{3}s/km	1	0.3	2
Internal state	Double streams	No double streams	?
	$T_{p\perp} > T_{p\parallel}$	$T_{p\perp} < T_{p\parallel}$	?
	$v_\alpha > v_p$	$v_\alpha \simeq v_p$	$v_\alpha \simeq v_p$
	$T_\alpha / T_p > 4$	$T_\alpha / T_p < 4$	?
	Strong strahl	Weak strahl	?

References

Bame, S. J., J. R. Asbridge, W. C. Feldman, and J. T. Gosling, Evidence for a structure-free state at high solar wind speeds, J. Geophys. Res., 82, 1487, 1977.

Bame, S. J., J. R. Asbridge, W. C. Feldman, E. E. Fenimore, and J. T. Gosling, Solar-wind heavy ions from flare-heated coronal plasma, Solar Phys., 62, 179, 1979.

Bame, S. J., J. R. Asbridge, W. C. Feldman, J. T. Gosling, and R. D. Zwickl, Bi-directional streaming of solar wind electrons 80 eV: ISEE evidence for a closed-field structure within the driver gas of an interplanetary shock, Geophys. Res. Lett., 8, 173, 1981.

Bavassano, B., M. Dobrowolny, and F. Mariani, Evidence of magnetic field line merging in the solar wind, J. Geophys. Res., 81, 1, 1976.

Borrini, G., J. T. Gosling, S. J. Bame, and W. C. Feldman, Helium abundance enhancements in the solar wind, J. Geophys. Res., 87, 7370, 1982.

Borrini, G., J. T. Gosling, S. J. Bame, W. C. Feldman, and J. M. Wilcox, Solar wind helium and hydrogen structure near the heliospheric current sheet: a signal of coronal streamers at 1 AU, J. Geophys. Res., 86, 4565, 1981.

Burlaga, L. F., K. W. Behannon, S. F. Hansen, G. W. Pneuman, and W. C. Feldman, Sources of magnetic fields in recurrent interplanetary streams, J. Geophys. Res., 83, 4177, 1978.

Feldman, W. C., J. R. Asbridge, S. J. Bame, and J. T. Gosling, High-speed solar wind flow parameters at 1 AU, J. Geophys. Res., 81, 5054, 1976.

Feldman, W. C., J. R. Asbridge, S. J. Bame, J. T. Gosling, and D. S. Lemons, Characteristic electron variations across simple high-speed solar wind streams, J. Geophys. Res., 83, 5285, 1978.

Feldman, W. C., J. R. Asbridge, S. J. Bame, E. E. Fenimore, and J. T. Gosling, The solar origins of solar wind interstream flows: near-equatorial coronal streamers, J. Geophys. Res., 86, 5408, 1981.

Fenimore, E. E., Solar wind flows associated with hot heavy ions, Astrophys. J., 235, 245, 1980.

Gosling, J. T., V. Pizzo, and S. J. Bame, Anomalously low proton temperatures in the solar wind following interplanetary shock waves -- evidence for magnetic bottles?, J. Geophys. Res., 78, 2001, 1973.

Hansen, S. F., C. Sawyer, and R. T. Hansen, K corona and magnetic sector boundaries, Geophys. Res. Lett., 1, 13, 1974.

Hirshberg, J., S. J. Bame, and D. E. Robbins, Solar flares and solar wind helium enrichments: July 1965 - July 1967, Solar Phys., 23, 467, 1972.

King, J. H., Interplanetary Medium Data Book, Rep. NSSDC 7704, NASA Goddard Space Flight Center, Greenbelt, MD, 1979.

King, J. H., Interplanetary Medium Data Book, Supplement 1, Rep. NSSDC 7904, NASA Goddard Space Flight Center, Greenbelt, MD, 1979.

Klein, L. W., and L. F. Burlaga, Interplanetary clouds at 1 AU, J. Geophys. Res., 87, 613, 1982.

Krieger, A. S., A. F. Timothy and E. C. Roelof, A coronal hole and its identification as the source of a high velocity solar wind stream, Solar Phys., 29, 505, 1973.

Krieger, A. S., A. F. Timothy, G. S. Vaiana, A. J. Lazarus, and J. D. Sullivan, X-ray observations of coronal holes and their relation to high velocity solar wind streams, Solar Wind Three, C.T. Russell, ed., p. 132, University of California, Los Angeles, 1974.

Levine, R. H., The relation of open magnetic structures to solar wind flow, J. Geophys. Res., 83, 4193, 1978.
Montgomery, M. D., J. R. Asbridge, S. J. Bame, and W. C. Feldman, Solar wind electron temperature depressions following some interplanetary shock waves: evidence for magnetic merging?, J. Geophys. Res., 79, 3103, 1974.
Munro, R. H., J. T. Gosling, E. Hildner, R. M. MacQueen, A. I. Poland, and C. L. Ross, The association of coronal mass ejection transients with other forms of solar activity, Solar Phys., 61, 201, 1979.
Ness, N. F., A. J. Hundhausen, and S. J. Bame, Observations of the interplanetary medium: Vela 3 and Imp 3, 1965-1967, J. Geophys. Res., 76, 6643, 1971.
Neugebauer, M., Measurements of the properties of solar wind parameters relevant to studies of its coronal origin, Space Sci. Rev., 33, 127, 1982.
Nolte, J. T., A. S. Krieger, A. F. Timothy, R. E. Gold, E. C. Roelof, G. Vaiana, A. J. Lazarus, J. D. Sullivan, and P. S. McIntosh, Coronal Holes as sources of solar wind, Solar Phys., 46, 303, 1976.
Palmer, I. D., F. R. Allum, and S. Singer, Bidirectional anisotropies in solar cosmic ray events: evidence for magnetic bottles, J. Geophys. Res., 83, 75, 1978.
Pilipp, W. G., R. Schwenn, E. Marsch, K.-H. Muhlhauser, and H. Rosenbauer, Electron characteristics in the solar wind as deduced from Helios observations, Solar Wind Four, H. Rosenbauer, ed., Max-Planck-Institut fur Aeronomie Report MPAE-W-100-81-31, p. 241, Katlenburg-Lindau, 1981.
Rosenbauer, H., R. Schwenn, E. Marsch, B. Meyer, H. Miggenrieder, M. D. Montgomery, K. H. Muhlhauser, W. Pilipp, W. Voges, and S. M. Zink, A survey on initial results of the Helios plasma experiment, J. Geophys. Res., 42, 561, 1977.
Schwenn, R., M. D. Montgomery, H. Rosenbauer, H. Miggenrieder, K. H. Muhlhauser, S. J. Bame, W. C. Feldman, and R. T. Hansen, Direct observations of the latitudinal extent of a high speed stream in the solar wind, J. Geophys. Res., 83, 1011, 1978.
Schwenn, R., H. Rosenbauer, and K. H. Muhlhauser, Singly ionized helium in the driver gas of an interplanetary shock wave, Geophys. Res. Lett., 7, 201, 1980.
Steinitz, R., and M. Eyni, Global properties of the solar wind. 1. The invariance of the momentum flux density, Astrophys. J., 241, 417, 1980.
Steinitz, R., Y. Klemens, and M. Eyni, Momentum flux density of the solar wind: invariance and the solar cycle, preprint, 1982.
Wilcox, J. M., and N. F. Ness, Quasi-stationary corotating structure in the interplanetary medium, J. Geophys. Res., 70, 5793, 1965.
Zwickl, R. D., J. R. Asbridge, S. J. Bame, W. C. Feldman, and J. T. Gosling, He^+ and other unusual ions in the solar wind: a systematic search covering 1972-1980, J. Geophys. Res., 87, 7379, 1982.